Electronically Supplementary Information

Magnetic nanoparticles synthesis by laser ablation of strontium ferrite under water and their characterization by optically detected magnetophoresis supported by BEM calculations

*Valentina Piotto,[a†] Lucio Litti,[a†] A. Omelyanchik,[b] Alessandro Martucci,[c] Piero Riello,[d] Davide Peddis,[b] Moreno Meneghetti [a]**

[a] Department of Chemical Sciences, University of Padova, via Marzolo 1, 35131 Padova, Italy, moreno.meneghetti@unipd.it

[b] Department of Chemistry and Industrial Chemistry, University of Genova, via Dodecaneso 31, 16146 Genova, Italy

[c] Department of Industrial Engineering, University of Padova, Via Marzolo, 35131 Padova, Italy

[d] Department of Molecular Sciences and Nanosystems, Università Ca' Foscari Venezia, 30170 Mestre, Venezia, Italy

1) Brownian motion of nanoparticles

The probability of the time dependent position of nanoparticles subject to a Brownian motion can be described with the following gaussian distribution:

$$f(z) = \frac{1}{\sqrt{2\pi\sigma^2}} \cdot e^{-\frac{(z-\mu)^2}{2\sigma^2}}$$

where $\sigma^2=2Dt$, D is the diffusion coefficient and μ the mean position of the distribution. The distribution has a time dependence, which means that it widens with time (see **Errore. L'origine riferimento non è stata trovata.** S1).

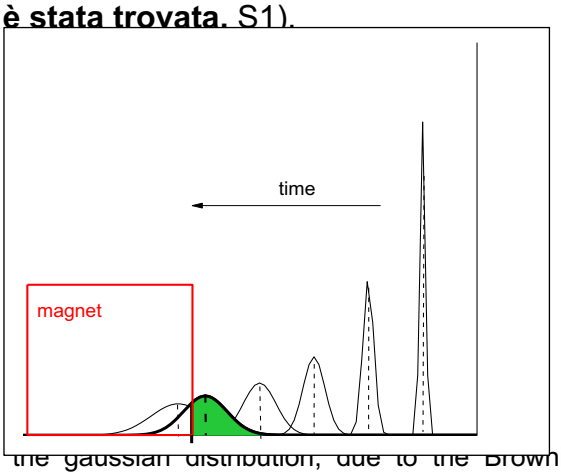

Figure S1. Time widening of the gaussian distribution, due to the Brownian motion, of magnetic nanoparticles attracted by a magnet. The part of the gaussian distribution that is still in solution for a nanoparticle whose mean position μ has not already reached the magnet is evidenced in green.

In Figure S1 one can appreciate that the front of the distribution is not present in solution also when the mean position of a nanoparticle does not reach the magnet surface. The same happens when the mean position is found after the magnet surface. In this case the tail continues to be in solution. Considering that nanoparticles are homogenously distributed in the solution and that they start their motion toward the magnet surface at different distances, one can predict a compensation of tails and fronts of the distribution of particles reaching the magnet at different times. To show the presence of the compensation, magnetophoretic curves which consider ('BR YES') or not ('BR NO') the presence of the Brownian motion are reported in Figure S2. The diffusion coefficient for spherical particles is given by the Stokes-Einstein equation $D=k_BT/(6\pi\eta r)$, where T is the temperature, η is the viscosity, r the radius of the particle and k_B the Boltzman constant. The Brownian motion becomes important in particular for small particles, being the diffusion dependent on the inverse of the nanoparticle radius. To show a situation which can be critical, we considered ideal nanoparticles with small diameters and the distribution reported in Figure S2a. Their size dependent extinction is reported in Figures 1. The simulated magnetophoretic experiment was performed

considering the set-up (magnet, optical path and larger distance the nanoparticle can travel) used in the paper.

Figure S2b reports the two calculated magnetophoretic curves and one can see that they are almost identical and small differences are found only at long times.

Increasing the radius of the nanoparticles and, therefore, decreasing the total time of the magnetophoretic experiment, the differences almost vanish.

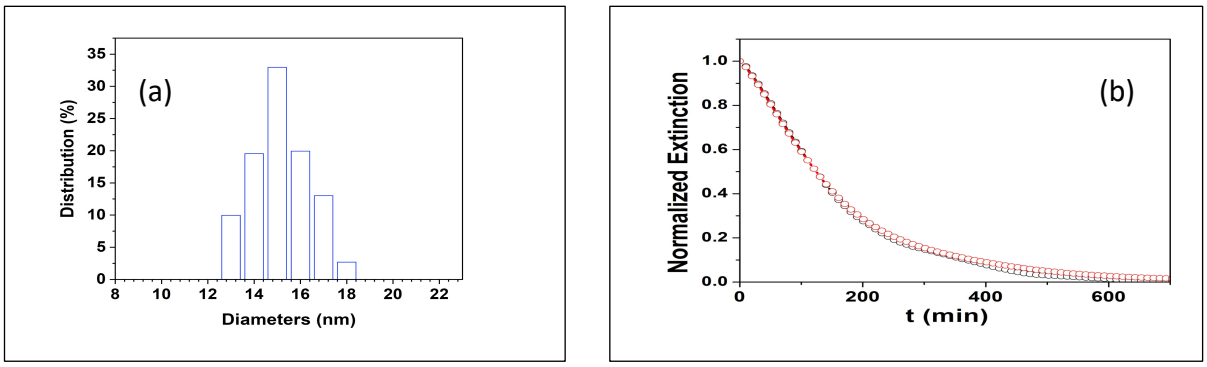

Figure S2. Calculated magnetophoretic curve (b) with (BR YES, red circle) or without (BR NO, black circle) the Brownian contribution for nanoparticles with the distribution reported in (a).

An important geometric characteristic of the magnetophoretic experiment is the larger distance a nanoparticle can travel. In Figure S3 a comparison is made for a decreasing space (from 3 mm to 1 mm) the nanoparticle has to travel toward the magnet surface.

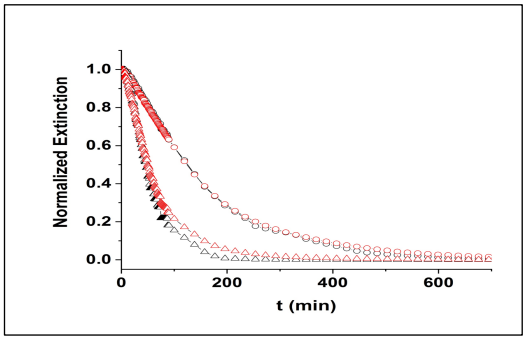

Figure S3. Calculated magnetophoretic curve considering (BR YES, red symbols) or not (BR NO, black symbols) the Brownian contribution for a sample of HiQ-Nano nanoparticles starting their motion at maximum from 1 mm (triangles), or 3 mm (circles) from the magnet.

The calculated curves show that increasing the distance from the magnet the Brownian motion has a minor influence. One can conclude that the Brownian motion can be important for very small nanoparticles with maximum travel distance not far from the magnetic surface and that for the experiments reported in the present work it has a minor influence.

2) BEM Results

BEM calculations allow to obtain the absorption and scattering contributions to the extinction spectrum of nanoparticles. Figure S4 a and b report the absorption contribution of nanoparticles of magnetite of dimensions from 10 nm to 500 nm. In Figure S4 c and d are reported the corresponding curves for the scattering contribution.

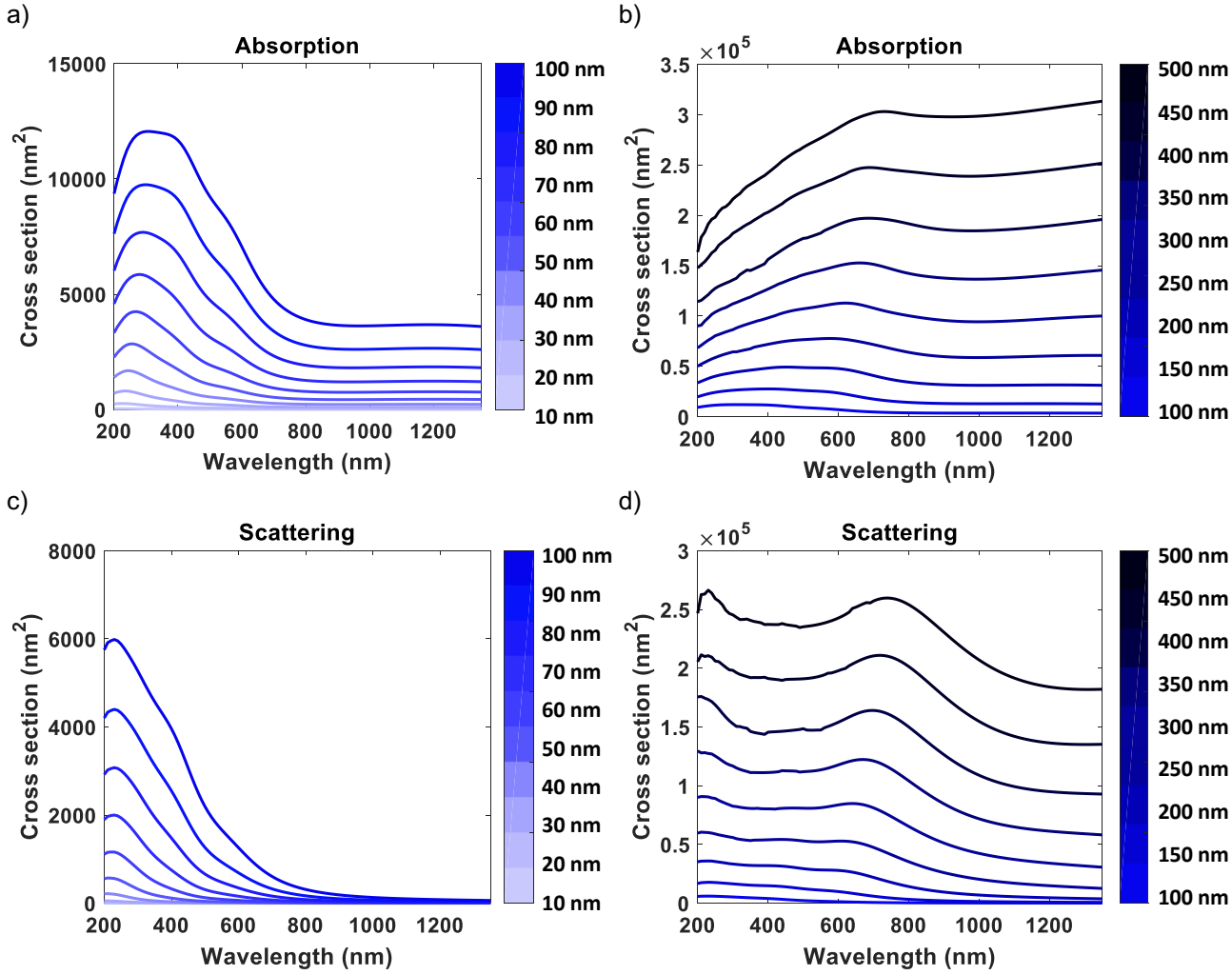

Figure S4. (a and b) BEM calculated absorption spectra for magnetite nanoparticles with diameters from 10 to 100 nm (a) and from 100 to 500 nm (b); (c and d) BEM calculated scattering spectra for magnetite nanoparticles with diameters from 10 to 100 nm (c) and from 100 to 500 nm (d).

3) Magnetic characterization of the S-10-20-N magnet

The magnetic field of the S-10-20-N magnet was determined within 3 mm from its surface (z coordinate) with a Lake Shore Gaussmeter. Figure S5a shows the recorded magnetic field at z=0 on the surface of the magnet. Values of the magnetic field vary from 0.55 T on the surface of the magnet to 0.24 T at 3 mm from this surface. In Figure S5b is reported the

magnetic field gradient, with a maximum value of 115 T/m near the magnet surface and slow decreasing values along z within the first 3 mm.

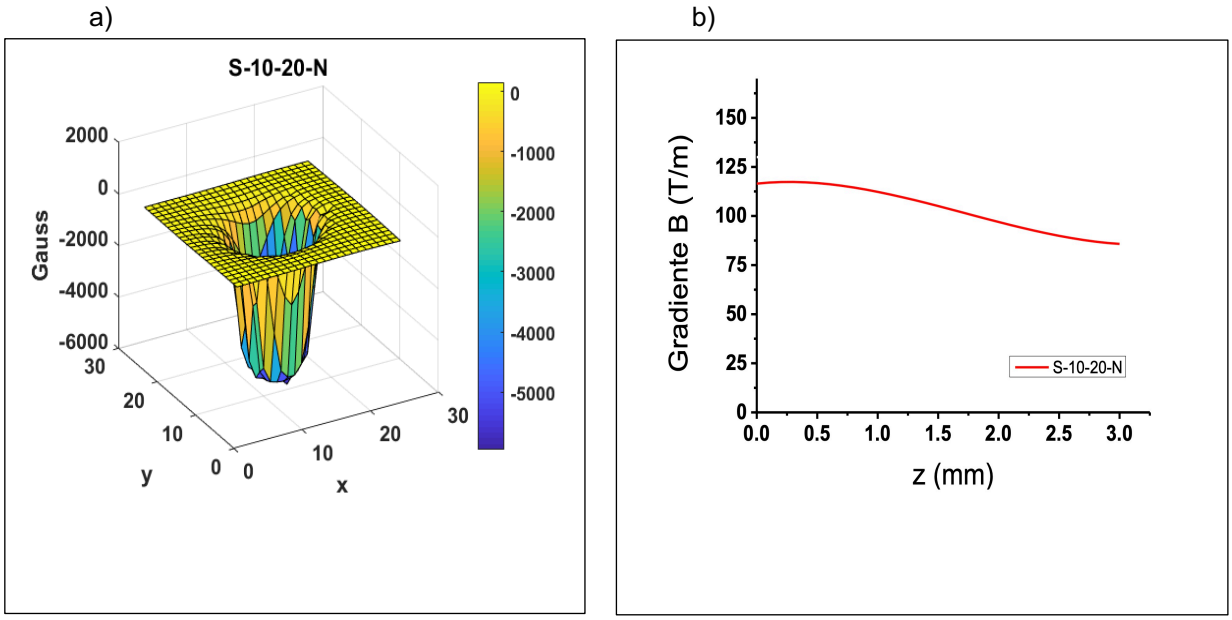

Figure S5. (a) Magnetic field of the S-10-20-N magnet measured with a Lake Shore Gaussmeter on the face on the magnet (z=0 mm). (b) Magnetic field gradient of the magnet calculated along z-axis.

4) Magnetic dipole interactions

The dipolar interaction can be neglected in the magnetophoretic model when the dilution and/or the thermal energy are sufficiently high. The parameter N* can be used for the evaluation of the interaction among dipole moments of the magnetic nanoparticles.[1] When the value of this parameter is lower than 1 the nanoparticles can be considered independent. For the ablated nanoparticles with 80 nm average dimension and the magnetization of saturation for magnetite the parameter N* is calculated to be 0.003 for the concentration of 80 mg L^{-1}, used for the magnetophoretic experiment This suggests that at this concentration the magnetic dipolar interaction can be neglected.

5) Raman and EDX characterization of the laser ablated nanoparticles

The Raman analysis of the ablated sample is reported in Figure S6a.

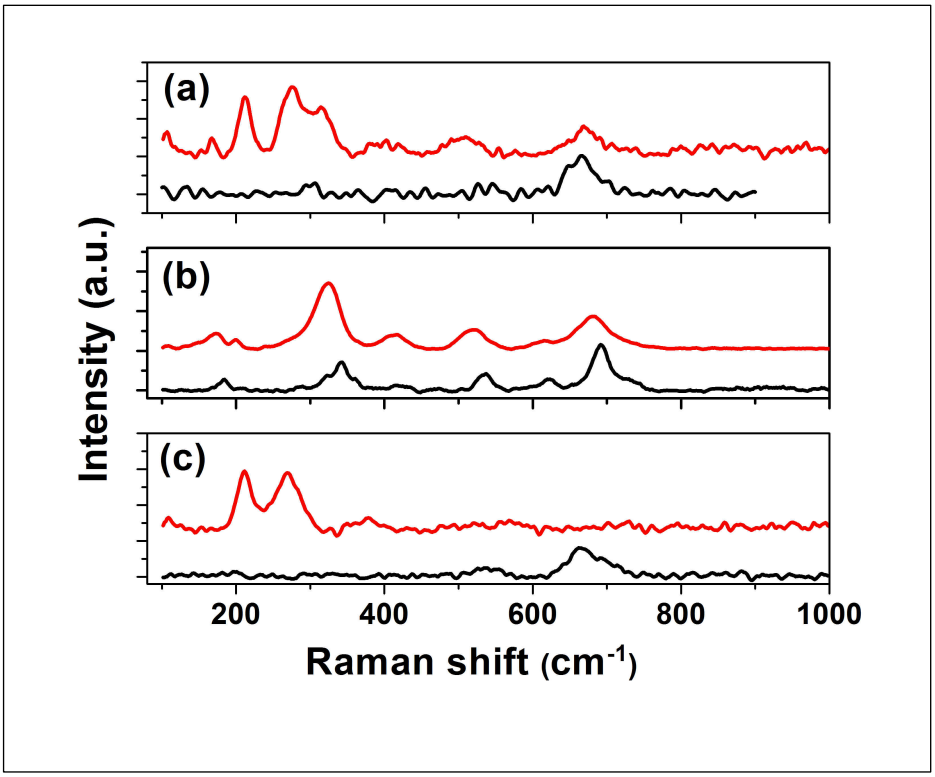

Figure S6. Raman spectra excited at 514 nm at low laser power (0.5 mW, 20x objective, black lines) and high laser power (25 mW, 20x objective, red lines). (a) spectra of the ablated material (b) reference spectra of the strontium ferrite bulk material; (c) reference spectra of magnetite

The Raman spectra of the ablated material (Fig. S6a) recorded with a laser at low power(black line) and recorded after exposing the sample at high power (red line), can be interpreted by comparison with the corresponding spectra of strontium ferrite (Fig. S6b) and of magnetite (Fig. S6c).

In the spectrum of the ablated material (Fig. S6a, black line) recorded with a laser at low power one can see only a broad band around 680 cm^{-1}, which can be attributed to magnetite and strontium ferrite. However, one can see that magnetite recorded after exposing the sample at high laser power completely transforms into hematite (Fig. S6c, red line) characterized by two bands at 214 and 276 cm^{-1}.[2] This transformation is not observed for strontium ferrite (Fig. S6b). The Raman spectrum of the ablated material recorded after exposing the sample at high power laser (Fig. S6a, red line) shows the bands of hematite, but a band at about 670 cm^{-1} is always present together with others which, by comparison,

are found in the spectrum of strontium ferrite. Therefore, one can conclude that in the ablated material are present both magnetite and strontium ferrite.

EDX measurement was used for evaluating the relative abundance of the elements in the ablated material.

The material was deposited by drop casting on a Ge slide to avoid interferences with the peaks of Fe and Sr, and the EDX spectra, recorded for two cluster of nanoparticles, as reported in Figure S7, using an incident electron beam at 20 keV, are reported in Figure S8. The analysis of the spectra are reported in Table S1. The atom ratio between Fe and Sr was found to be, on average, 27±1 by using calibrated signals for the peak of Fe $(K_{\alpha 1}, K_{\alpha 2})$ at 6.40 keV and that of Sr $(L_{\alpha 1}, L_{\alpha 2}, L_{\beta})$ at 1.83 keV.

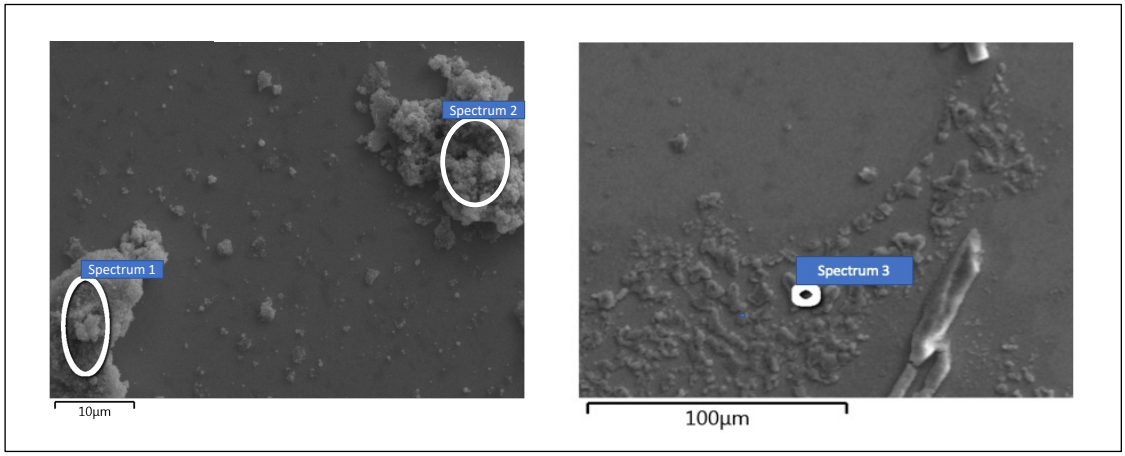

Figure S7. SEM image of the ablated nanoparticles where the EDX spectra were recorded.

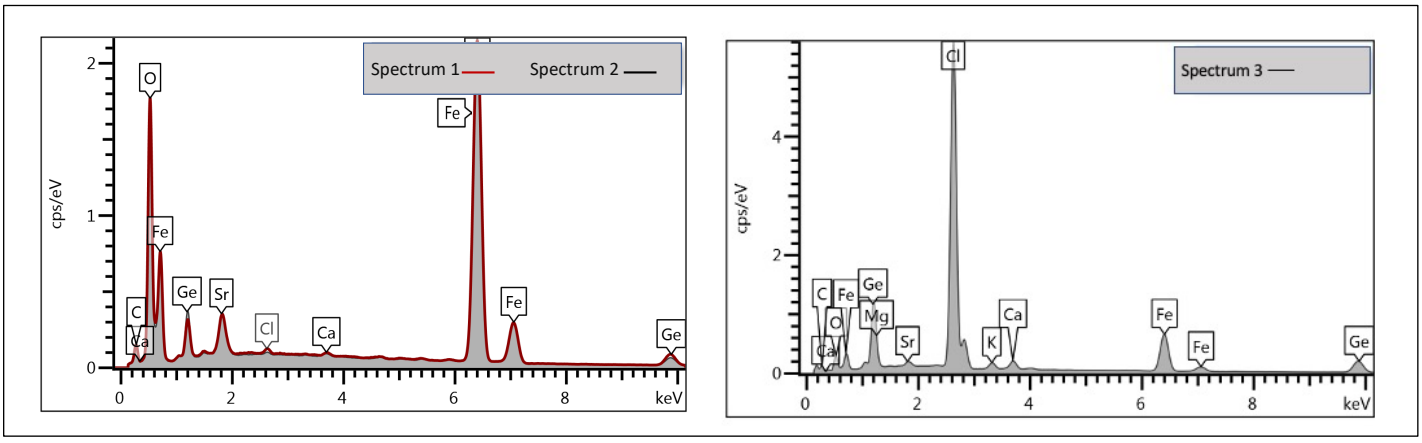

Figure S8. EDX spectra of the laser ablated nanoparticles for two measurements obtained for two clusters of nanoparticles (see Figure S7).

Spectrum label	Spectrum 1	Spectrum 2	Spectrum 3
C	16.48	16.63	54.93
O	49.28	47.04	14.14
Mg			0.75
Cl	0.23		19.69
K			0.49
Ca	0.17	0.12	0.66
Fe	30.43	31.89	5.59
Ge	2.33	3.06	3.55
Sr	1.08	1.25	0.20
Total	100.00	100.00	100.00

Table S1. Analysis of the EDX spectra reported in Figure S8.

6) Scheme of the magnetophoretic cell

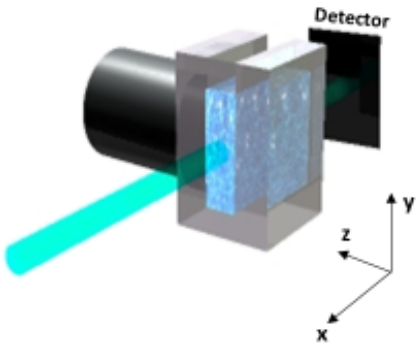

Figure S9. Scheme of the magnetophoretic cell with the magnet on the left side of the cell and the beam entering the front of the cell and reaching the detector after the cell.

1. Faraudo, J.; Andreu, J. S.; Calero, C.; Camacho, J., Predicting the Self-Assembly of Superparamagnetic Colloids under Magnetic Fields. *Advanced Functional Materials* **2016,** *26* (22), 3837-3858.

2. Balcells, L.; Martinez-Boubeta, C.; Cisneros-Fernandez, J.; Simeonidis, K.; Bozzo, B.; Oro-Sole, J.; Bagues, N.; Arbiol, J.; Mestres, N.; Martinez, B., One-Step Route to Iron Oxide Hollow Nanocuboids by Cluster Condensation: Implementation in Water Remediation Technology. *Acs Applied Materials & Interfaces* **2016,** *8* (42), 28599-28606.